

Article

Simulation-Based Exceedance Probability Curves to Assess the Economic Impact of Storm Surge Inundations due to Climate Change: A Case Study in Ise Bay, Japan

Xinyu Jiang ¹, Nobuhito Mori ², Hirokazu Tatano ² and Lijiao Yang ^{1,*}

¹ School of Management, Wuhan University of Technology, Wuhan 430070, China; jxy119@163.com

² Disaster Prevention Research Institute, Kyoto University, Kyoto 6110011, Japan; mori@oceanwave.jp (N.M.); tatano.hirokazu.7s@kyoto-u.ac.jp (H.T.)

* Correspondence: Yanglj976@163.com

Received: 1 January 2019; Accepted: 15 February 2019; Published: 19 February 2019



Abstract: Understanding storm surge inundation risk is essential for developing countermeasures and adaptation strategies for tackling climate change. Consistent assessment of storm surge inundation risk that links probability of hazard occurrence to distribution of economic consequence are scarce due to the lack of historical data and uncertainty of climate change, especially at local scales. This paper proposes a simulation-based method to construct exceedance probability (EP) curves for representing storm surge risk and identifying the economic impact of climate change in the coastal areas of Ise Bay, Japan. The region-specific exceedance probability curves show that risk could be different among different districts. The industry-specific exceedance probability curves show that manufacturing, transport and postal activities, electricity, gas, heat supply and water, and wholesale and retail trade are the most affected sectors in terms of property damage. Services also need to be of concern in terms of business interruption loss. Exceedance probability curves provide complete risk information and our simulation-based approach can contribute to a better understanding of storm surge risk, improve the quantitative assessment of the climate change-driven impacts on coastal areas, and identify vulnerable regions and industrial sectors in detail.

Keywords: exceedance probability curves; storm surge inundation; climate change; economic impact; Ise Bay

1. Introduction

Between 1998 and 2017, disaster-hit countries reported direct economic losses amounting to US\$ 2908 billion, of which climate-related disasters caused 77% of the total damages. Storms cost more than any other climate-related disaster in high- and low-income countries, accounting for 75% and 61% of their reported losses, respectively [1]. The risk of storm disasters is likely to increase with climate change. On one hand, hazards of tropical cyclones are expected to increase in intensity owing to warmer sea surfaces, although their frequency is expected to decrease [2]. On the other hand, exposure of population in low-lying coastal areas, which is particularly vulnerable to storm disasters, is expected to increase and in Asia alone, is predicted to reach 695 million by 2030 (up from the baseline of 460 million in 2000) [3].

Understanding disaster risk, which was emphasized in the Sendai framework, should be a priority to achieve disaster risk reduction in the next 15 years [4]. Risk is a function of hazard, exposure, and vulnerability [5]. However, for natural disasters, many studies have focused on only hazard prediction [6–8] and have followed a hazard-projection–hazard-countermeasure decision process [9]. The concept of risk

in natural disasters emphasizes the integration of hazard, exposure, and vulnerability, and promotes the decision process of hazard-projection-social impact evaluation–risk-estimation–risk-countermeasures. For coastal regions, the risk from tropical storm surge inundation is responsible for most of the damage and loss [10–12] and is projected to worsen as coastal cities grow and the natural environment changes [13,14]. To estimate storm surge inundation risk, it is necessary to consider climate change scenarios [15–17]. Although previous studies have focused on assessing storm surge inundation risk in terms of hazard prediction [18–20], there is little information on risk assessment that integrates storm surge inundation hazard, exposure, and vulnerability because of climate change.

Risk can be expressed relatively as an overall, quantitative index that integrates contributing factors [21–24]. However, the index is sometimes not enough for decision making. The actions needed for reducing storm surge risk include countermeasures that range from disaster prevention to risk transfer, and for achieving the right balance among these countermeasures, a complete expression of risk is required. Risk; therefore, should be expressed as a curve that describes the probability and severity of adverse effects [25]. Haimes pointed out two ways of interpreting this definition: (i) The risk that describes the probability of occurrence of adverse effects; and (ii) the risk that describes the probability of the severity of adverse effects given their occurrence [26–28]. In terms of storm surge inundation risk, the former interpretation emphasizes the probability distribution of a storm surge inundation hazard, and the latter focuses on the probability of economic loss caused by storm surge inundation. However, the knowledge of the probability of both the hazard and the corresponding economic loss is essential to deal with the associated risk.

An exceedance probability (EP) curve is a type of risk curve that may integrate the probability of hazard and the corresponding economic loss. It describes the probability of economic loss exceeding a certain threshold. The advantage of using EP curves in climate change adaptation is that governments, companies, or individuals can use it to quantify the risk profile for entire portfolios or for individual risks, which can be region- or industry-specific. EP curves can help determine the quantum of risk to deal with in risk-control measures, and to assess how much to transfer by risk finance measures. An EP curve can be calculated from historical loss data using statistical methods. There are two difficulties associated with using historical loss data for storm surge inundation. Firstly, storm surge inundations are rare events and it is difficult to obtain adequate historical economic loss data for a specific area. Secondly, the influence of climate change cannot be captured by only analyzing the historical data.

Therefore, to assess the economic impact of storm surge inundation due to climate change, a method of simulation-based EP curve construction is proposed and a case study is conducted to demonstrate this methodology. The remainder of this paper is structured as follows. Section 2 introduces the study area, describes an EP curve, and the methodology framework to construct it. Section 3 presents the results from the case study using the proposed method. The discussions and conclusions are presented in Sections 4 and 5.

2. Methods

2.1. Study Area

The study area, Ise Bay, is in central Japan. Ise Bay is contiguous with three prefectures, but most of our study area was in the Aichi prefecture. The capital of Aichi prefecture, Nagoya city, is the third largest city in Japan, after Tokyo and Osaka. This area primarily focuses on automobiles, with a large concentration of industries in aircraft, space, and machine tools. Many world-famous companies, like Toyota, Fuji Heavy Industries, Mitsubishi Motors Corporation, Brother Industries Ltd., Aisin Seiki Co. Ltd, are located in this area. Ise Bay is the gateway to the Nagoya economic zone. This area is considered vulnerable to storm surge inundation. In 1959, typhoon Vera attacked this area and caused the most severe historical storm surge disaster in Japan. The location of the case study area is shown in Figure 1.

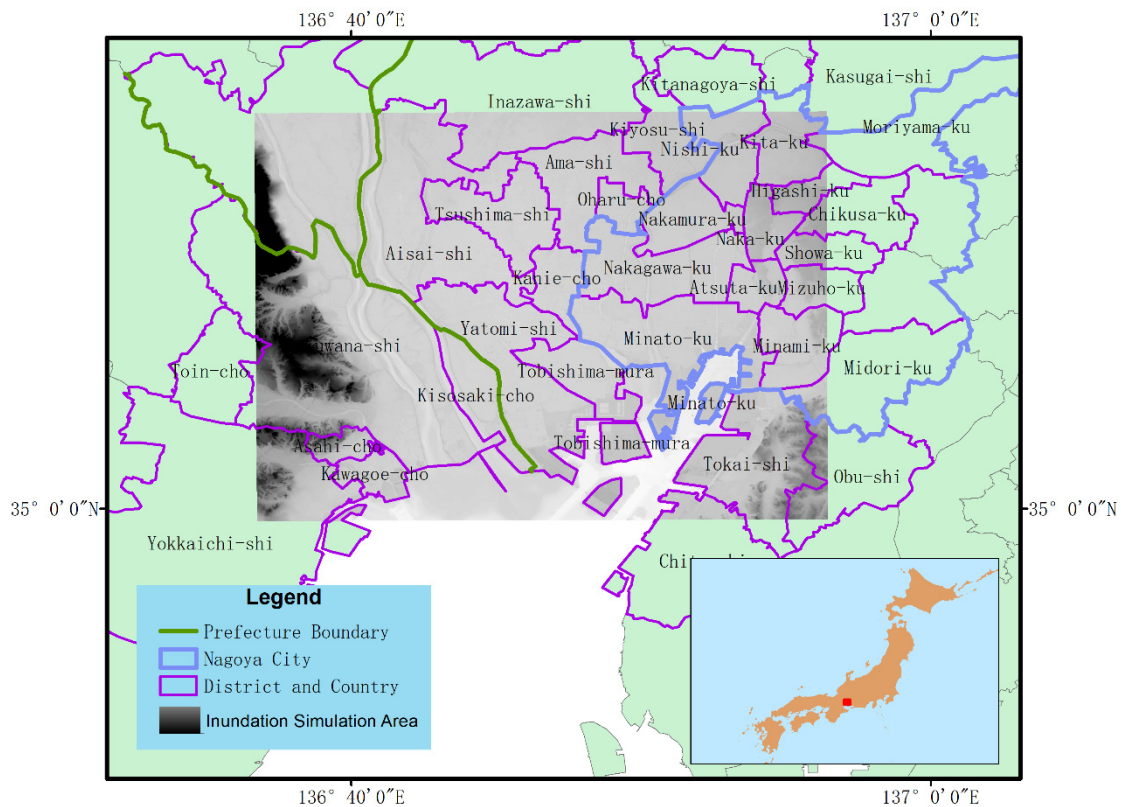


Figure 1. Case study area.

2.2. Methodology

2.2.1. Exceedance Probability Curves

The construction of the EP curves using simulation data is illustrated by Figure 2. A dot in the figure represented a loss value caused by a typhoon storm surge inundation case. The dots connected by a light dashed line was from the same typhoon ensemble. Each typhoon ensemble provided a set of storm surge inundation losses with probabilities. Therefore, at a certain probability of typhoon occurrence, several loss values could be estimated. The probability distribution of such loss values represented the variation in loss caused by the uncertainty of a typhoon for a specific probability. Here, the exceedance probability of loss was linked to the probability of the occurrence of a typhoon under ensemble forecasting.

Assuming λ is the probability of the occurrence of a typhoon and $f_{\lambda}(x)$ is the probability distribution of loss at typhoon occurrence probability λ , the exceedance probability $EP(x)$ of loss x can be estimated by integrating the shadow area $\int_x^{\infty} f_{\lambda}(x)d(x)$ over the domain of typhoon occurrence probability λ . The expression is shown in Equation (1).

$$EP(x) = \int_0^1 \lambda \times \int_x^{\infty} f_{\lambda}(x)d(x)d(\lambda) \quad (1)$$

Since sometimes we only focus on the significant probabilities of occurrence, such as 1/200, 1/100, 1/50, 1/20, etc., a discrete type of formula is presented in Equation (2), which can better explain Figure 2.

$$EP(x) = \sum_i (\lambda_i - \lambda_{i-1}) \times \int_x^{\infty} f_{\lambda_i}(x)d(x) \quad (2)$$

where i represents the number of probabilities considered.

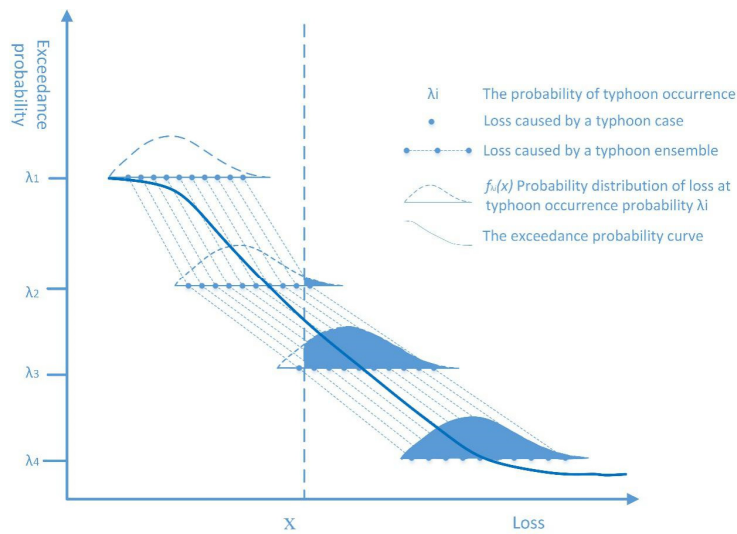


Figure 2. Illustration of simulation-based exceedance probability curve.

To obtain an EP curve for storm surge inundation, a framework was proposed in Figure 3 that included the following:

1. Hazard simulation. Using a statistical typhoon model to generate a large number of typhoon ensembles considering the characteristics of tropical cyclones captured by global circulation simulation under different climate conditions. Simulate the process of typhoon storm surge inundation for each typhoon case in the ensembles using a nested downscaling strategy and request a high-resolution simulation for inland inundation, as shown in Section 2.2.2.
2. Loss estimation. The estimation of losses for each storm surge inundation case with the integration of hazard, exposure, and vulnerability. Exposure can be divided into different categories and vulnerability is represented by the fragility curves of these exposure categories. Loss can be estimated in terms of property damage and business interruption losses, as presented in Section 2.2.3.
3. Estimation of EP curves. Plot the loss data of each ensemble according to the probability of typhoon occurrence and estimate the distribution of loss at each typhoon occurrence probability. Calculate EP curve using Formulas (1) or (2).

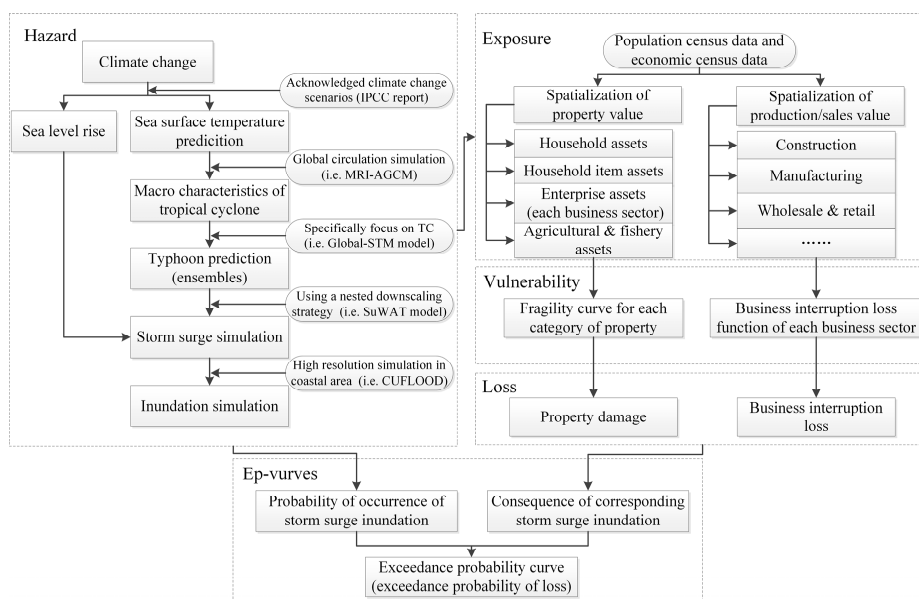


Figure 3. Methodology framework to estimate exceedance probability curves for storm surge inundation.

2.2.2. Prediction of Hazard under Climate Change

a) Prediction of Typhoon Hazard

Typhoon hazards can be predicted with a comprehensive application of global circulation models, downscaling methods, and simulation technologies [29–31]. The projection of climate change, such as change in sea surface temperature (SST), has been addressed by The Fourth and Fifth Assessment Report of IPCC. Based on the change in SST, climate conditions can be simulated using the super-resolution Atmospheric Global Circulation Model (AGCM) [32,33]. Using the results of climate condition simulation, Mori et al. analyzed the macro characteristics of tropical cyclones due to global climate change (e.g., the location of cyclogenesis) [16]. One of the findings of the study was that the average central pressure of a typhoon is expected to decrease to 30 hPa in the future depending on the greenhouse gases emissions, Global Circulation Model (GCM) performance, and latitude. Further, considering the tropical cyclone characteristics, a global scale stochastic tropical cyclone model (Global-STM) is developed and used to generate synthetic typhoon tracks [34]. Although GCM projection is useful to understand dynamic climatological change, the number of typhoons is insufficient to analyze the extreme regional changes due to climate change. A number of synthetic tropical cyclones considering the present and future climate conditions can be generated by the Global-STM at a global scale, as compared to from the GCM projections. Typhoons under present climate conditions were generated for 200 years. To understand the uncertainty of climate change, 25 typhoon ensembles were generated. In this study, the total number of typhoons generated in the Western Pacific Ocean was 563,727. The future typhoon hazards were generated by decreasing the central pressure of the present typhoons. Since our focus was on the storm surge inundation in Ise Bay, the significant synthetic tropical cyclones were selected using the following criteria to avoid unnecessary inundation simulations. The selection criteria used was: (1) The minimum distance to Ise Bay was less than 100 km; (2) the minimum central pressure was less than 950 hPa; and (3) the velocity of the tropical cyclone at landfall was higher than 20 km/h. Apart from the typhoon characteristics, the rise in sea level was also considered. According to IPCC, the global mean sea level is expected to rise 0.82 m in representative concentration pathway 8.5 (RCP8.5). Therefore, the current climate conditions and the future climate conditions for storm surge inundations were determined using the decreasing central pressure of typhoons and the rising sea level. Four climate scenarios were considered in this paper: (1) No decrease in central pressure, no rise in sea level; (2) a 10 hPa decrease in central pressure, a rise of 0.82 m in sea level; (3) a 20 hPa decrease in central pressure, a rise of 0.82 m in sea level; and (4) a 30 hPa decrease in central pressure, a rise of 0.82 m in sea level. The description of the climate change scenarios in the study is summarized in Table 1.

Table 1. Description of climate change scenarios in the study.

Climate Change Scenarios	Description	Number of Typhoon Ensembles	Years of Simulation
Present climate condition	No central pressure decrease; no sea level rise	25	200
Scenario 1	Central pressure decrease of 10 hPa; sea level rise of 0.82 m	25	200
Scenario 2	Central pressure decrease of 20 hPa; sea level rise of 0.82 m	25	200
Scenario 3	Central pressure decrease of 30 hPa; sea level rise of 0.82 m	25	200

b) Simulation of Storm Surges and Coastal Inundation

Storm surge simulation was conducted using a full-coupled surge-wave-tide coupled model (SuWAT) developed by Kim et al. [35]. In the study, the SuWAT employed a nesting scheme and used three domains with spatial resolutions of 7290, 2430, and 810 m, downscaled from northwest Pacific

Ocean and Japan coast to Ise Bay [36]. The storm surges were simulated taking the typhoon cases generated by the probabilistic typhoon model as input conditions.

Coastal inundation simulation requires higher spatial resolution to cooperate with exposure data; therefore, a 30-m spatial resolution was used. With an increase in spatial resolution, the cost of simulation and time also increase. Since assessing the inundation risk requires simulating hundreds of storm surge scenarios, a Graphics processing unit (GPU)-based flood simulation model, CUDA accelerated Flooding Modeling System (CUFLOOD) developed by Liang et al. [37] was used to speed up the inland inundation simulation. In this study, CUFLOOD showed a distinct advantage in the repeated parameter calibration process and the large number of simulations. It enabled us to rapidly complete hundreds of inundation simulations that well support simulation-based risk assessment.

2.2.3. Economic Impact Analysis

a) Estimation of Property Damage

The estimation of property damage depends on data availability. In Japan, population census and economic census were conducted based on 500 m mesh resolution. This can be downscaled to a smaller scale with additional information, such as land use. All the population census and economic census data were spatialized using geographic information system (GIS). According to the Ministry of Land, Infrastructure, Transport and Tourism (MLIT) Japan, property can be categorized into six types—house assets, household item assets, depreciable assets of enterprises, inventory assets of enterprises, depreciable assets of agricultural and fishery activities, and inventory assets of agricultural and fishery activities. The value of these assets can be directly or indirectly evaluated from the census and economic census data under certain assumptions [38]. A group of commonly-used fragility curves in Japan that reveal the relationship between water depth and loss ratio for each category can be found in the Manual of Economic Survey for Water Management published by MLIT.

b) Estimation of Business Interruption Loss

The definition and significance of business interruption loss have been discussed by Chang, Rose, Hallegatte, and Kajitani [39–42]. Business interruption loss signifies the loss caused by the functionality damage of industry sectors. Based on the economic survey data taken after the Tokai flood of 2000 in Japan, Yang et al. estimated the business interruption loss functions that define business interruption loss as lost production in affected days, and describe the relationship between water depth and business interruption loss [43]. A set of business interruption loss functions for manufacturing and non-manufacturing and for small classification sectors, including raw materials manufacturing, processing and assembly manufacturing, livelihood related manufacturing, wholesale and retail trade, services, and construction were provided through the study. This paper employed Yang et al.'s business interruption loss functions to estimate the business interruption loss for the industry sectors consistent with Yang et al.'s small classification sectors. The business interruption loss functions of these sectors are adopted directly for the small industry sectors that were not estimated in Yang et al.'s study; the loss functions of manufacturing and non-manufacturing are replaced. Business interruption loss can be estimated given the inundation and industry sector related information.

3. Results

3.1. Hazard Simulation and Exposure Distribution

Storm surge inundations were simulated for all selected typhoon cases under the four climate scenarios. From the results of the inundation simulations, the distributions of hazard information could be obtained. Figure 4 shows the worst-case simulation in each climate scenario. By analyzing the four worst cases, the different severity levels in the climate scenarios could be captured at first glance. It can be found that the total inundated area will increase about 63%, 85%, and 111% under climate

change scenarios 1, 2, and 3, respectively, compared to the present climate condition. More specifically, under climate change scenario 1, the inundated area with water depth in 0–1 m increases by 3%, the inundated area with water depth in 1–2 m increases by 98%, the inundated area with water depth in 2–3 m increases by 223%, and the inundated area with water depth in >3 m increases by 934%. The numbers for climate change scenario 2 were 2%, 127%, 307%, and 1444%, respectively, and for climate change scenario 3 were 12%, 140%, 364%, 2258%, respectively. From these comparisons, we can conclude that climate change will significantly enlarge the inundated area of deep water.

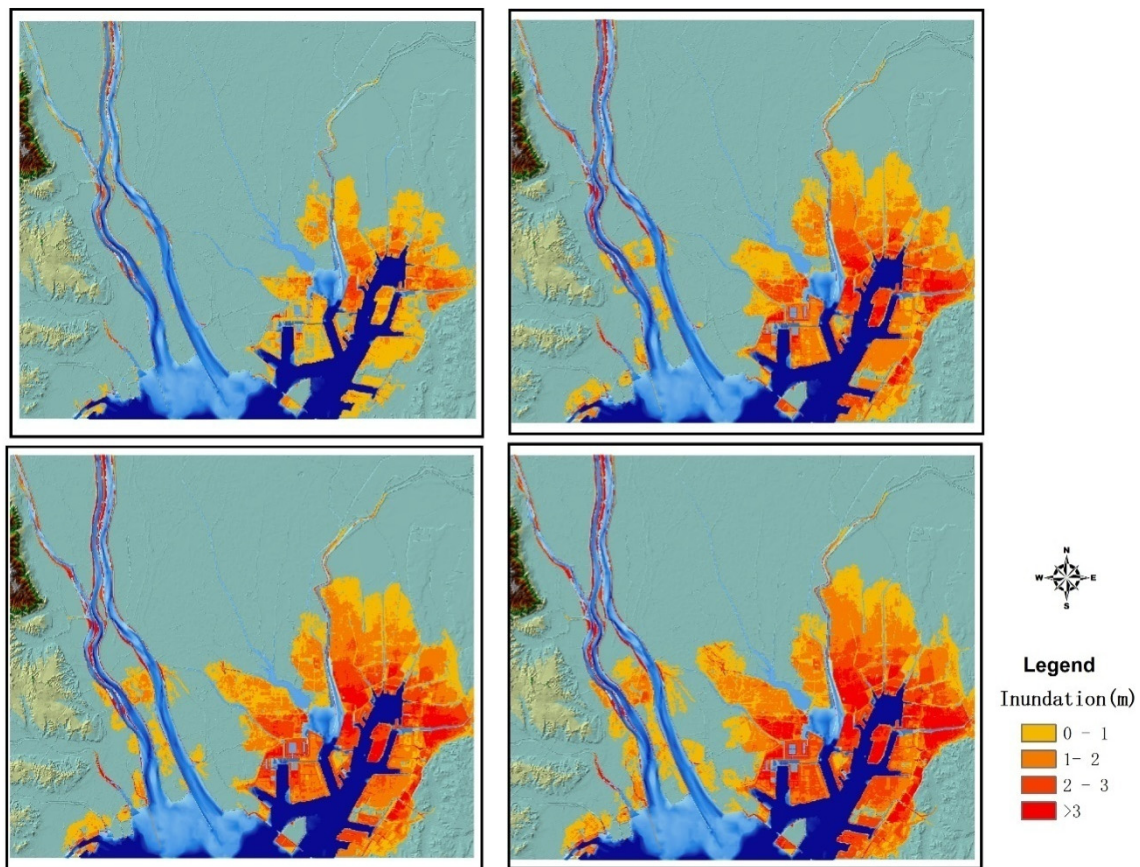


Figure 4. Worst-case storm surge inundation under different scenarios (Top left—no climate change; top right—climate change scenario 1; bottom left—climate change scenario 2; bottom right—climate change scenario 3).

The exposure data was spatialized at 100 m mesh scale. The property values were calculated based on the information of spatialized population, industry, land use, etc. Figure 5 shows examples of spatial distribution of total property value with information on land-use distribution and industry sector distribution. From the picture, the economy concentrated area could be identified, the right part of the study area was more developed and the property value was relatively higher. Similar spatial distributions of exposure for different specific property categories and industry sectors were obtained, which provided the basis for loss estimation and EP curve calculation.

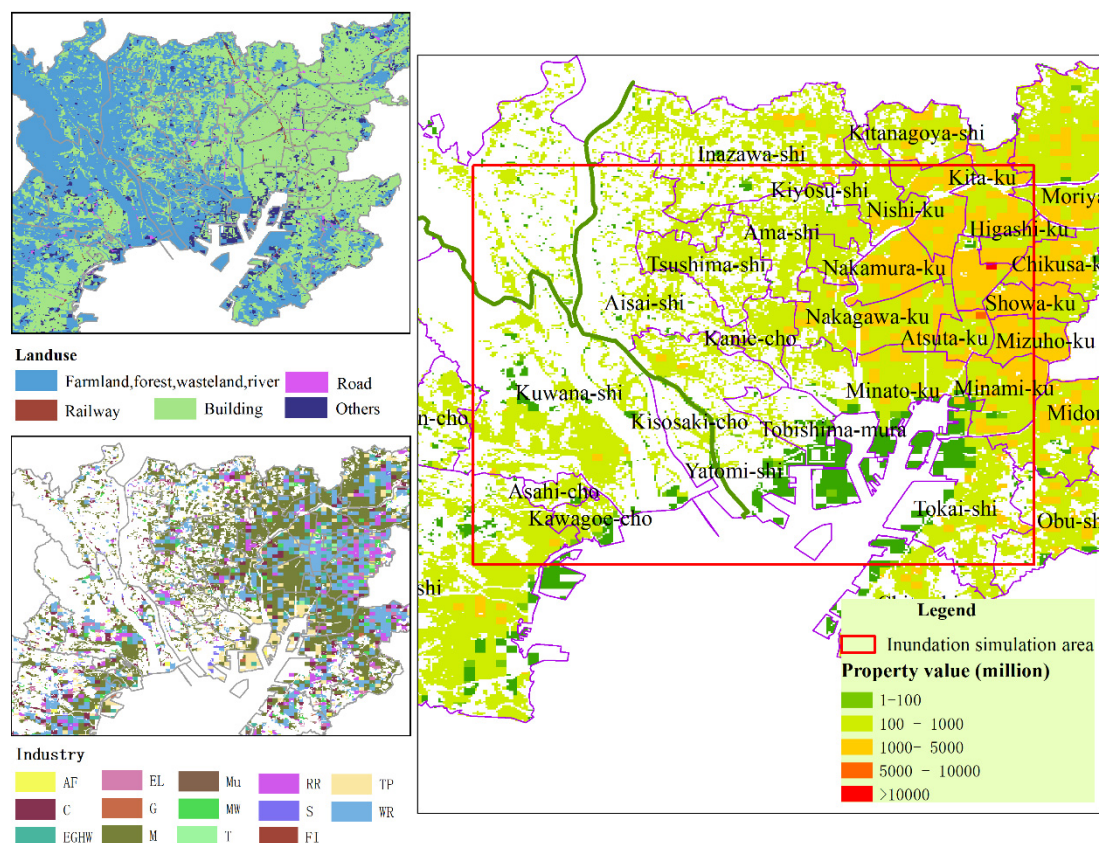


Figure 5. Spatial distribution of total property value with information of land-use distribution (top left) and industry sector distribution (bottom left). (C: Construction, M: Manufacturing, EGHW: Electricity, gas, heat supply, and water, T: Information and communications, TP: Transport and postal activities; WR: Wholesale and retail trade; FI: Finance and insurance; RR: Real estate and goods rental and leasing; AF: Accommodations, eating, and drinking services; EL: Education and learning support; MW: Medical, health care, and welfare; Mu: Multiservice; S: Services; G: Government affairs).

3.2. Estimation of EP Curves

3.2.1. Region-Specific EP Curves

Since both hazard and exposure information were spatially distributed, the estimation of economic loss and risk assessment could be conducted at basic mesh scales. However, to facilitate the discussion, loss estimation and risk assessment were aggregated to administrative region scales. Using the method presented in Section 2.2, region-specific EP curves were obtained. Figure 6 shows the EP curve of property damage for Nagoya city, where the Y-axis was the exceedance probability and the X-axis was the estimated property damage as a proportion of total value. Curves with different colors represent storm surge inundation risk under different climate change scenarios. One observation from the figure was that in Nagoya city, storm surge inundation risk increases with climate change. The impact of high-frequency storm surges, such as a 1/50 event, were not significantly different with or without climate change; however, the impact of low-frequency storm surges, such as a 1/200 event will dramatically increase under climate change scenarios.

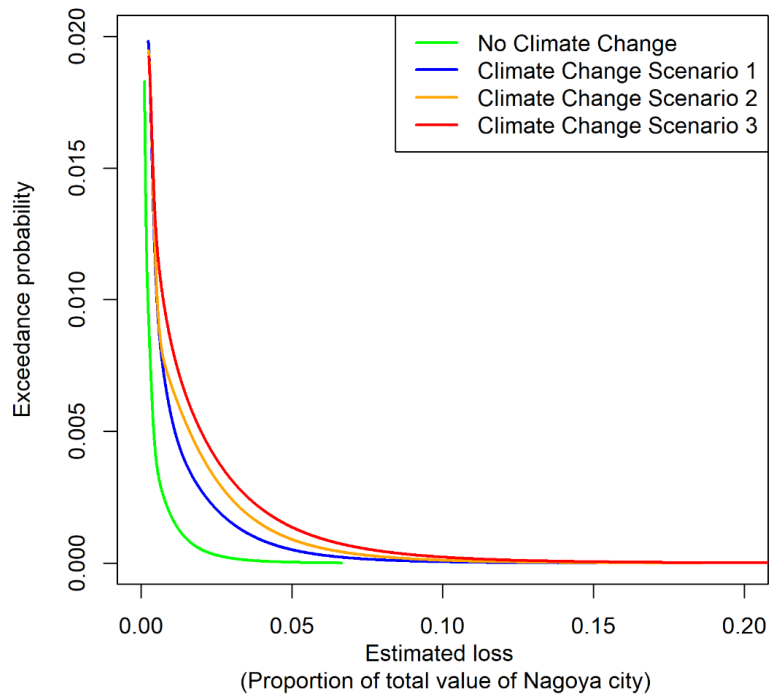


Figure 6. EP curves of property damage for Nagoya city under climate change scenarios.

3.2.2. Industry Sector-Specific EP Curves

The industry sector-specific EP curves were also obtained using the method outlined in Section 2.2. Figure 7 presents the EP curves of property damage for the manufacturing sector in Nagoya city under climate change scenarios. We found that the manufacturing sector was sensitive and highly susceptible to climate change. The green curve was the EP curve without climate change. It changed to blue, orange, and red under different climate change scenarios. Even for the high-frequency storm surges (1/50 event), the impact without and with climate change was significantly different.

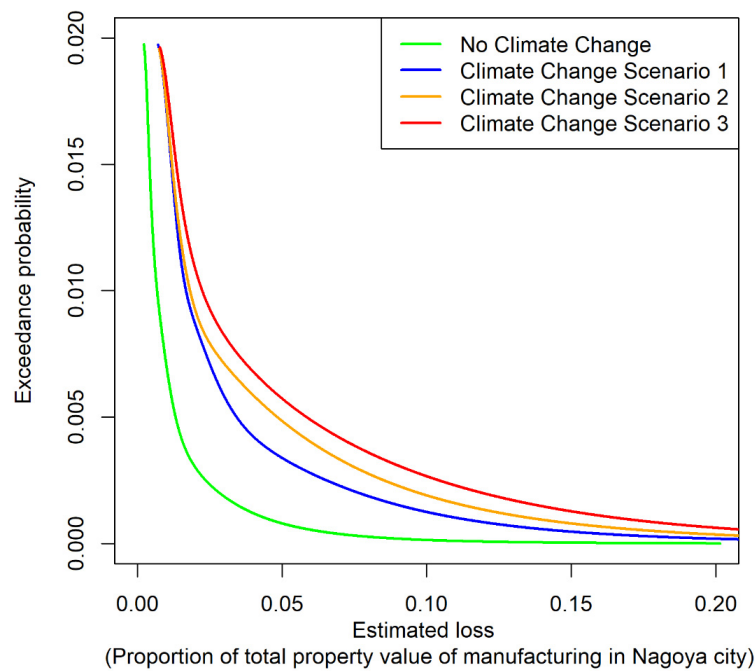


Figure 7. EP curves of property damage for the manufacturing sector in Nagoya city under climate change scenarios.

3.3. Application of EP Curves to Assess Economic Impacts

EP curves present the complete risk information on storm surges inundation. From the horizontal direction, the value at risk (VaR) could be obtained. Integrating the EP-curve, expected loss could be calculated. Comprehensively using region-specific and industry-specific EP curves, the economic impact of storm surge inundation caused by climate change could be properly evaluated. Three instances of the application of EP curves re elaborated in Sections 3.3.1–3.3.3.

3.3.1. Identification of Risky Areas

For each district, the EP curves under the four climate scenarios were estimated. Using the expected economic loss calculated from the EP curve as an index, the spatial distributions of risk were mapped, as shown in Figure 8. From the figure, it can be seen that there were two districts where the expected economic loss exceeded 500 million (Japanese yen) and three districts where the expected loss was between 100 and 500 million (Japanese Yen) under no climate change scenario. With climate change, the risk level in most districts increased and the number of districts where the expected economic loss would exceed 500 million (Japanese Yen) increased to five. More specifically, Minato district and Minami district were particularly vulnerable to a high storm surge risk, even without climate change, and the severity of the storm surge could be expected to increase with climate change. Nakagawa district, Midori district, and Tokai city became high-risk areas with climate change.

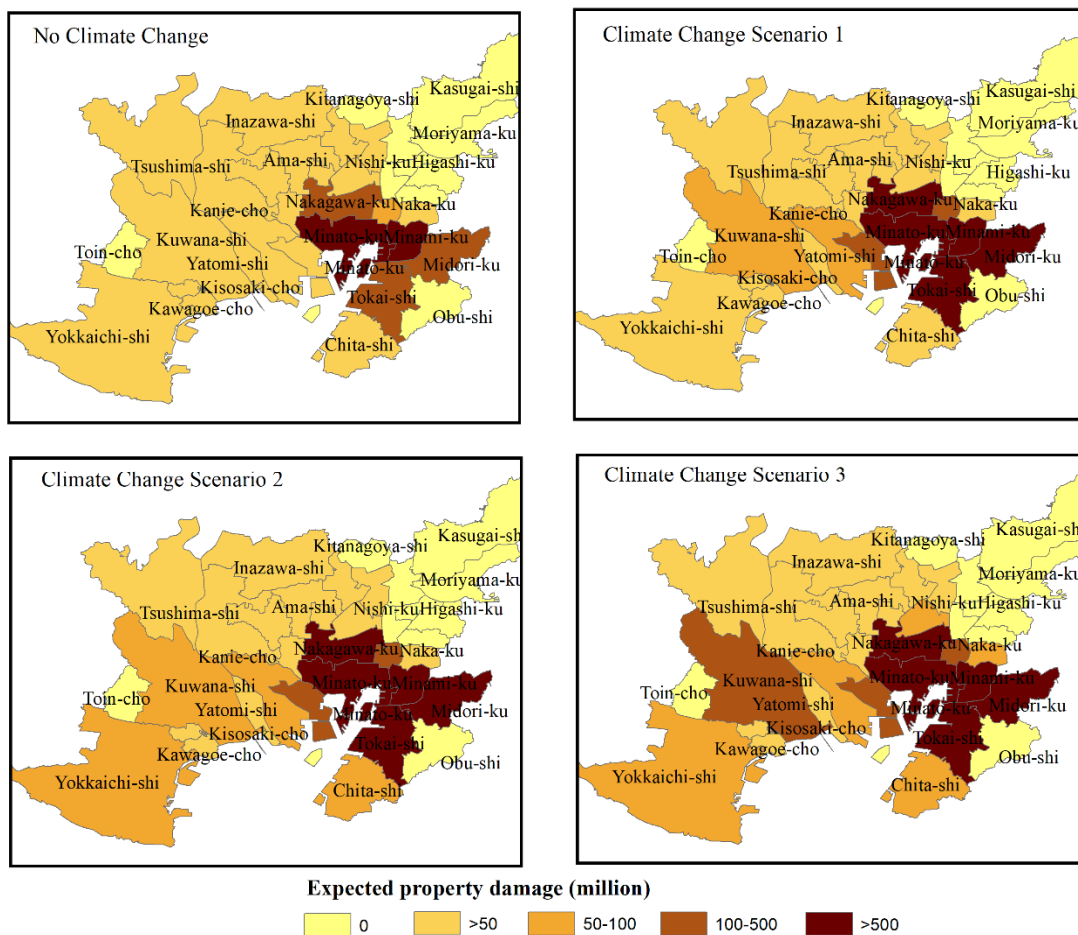


Figure 8. Risk maps of expected property damage under four climate change scenarios.

3.3.2. Identification of Vulnerable Industry Sectors

Using expected loss calculated from industry sector-specific EP curves as an index, radar maps were created to identify the storm surge risk to different industry sectors. Figure 9 presents an overview

of property damage and business interruption loss in Nagoya city. The inner-most circle denotes the base line of loss comparison. It denotes the value of the smallest expected economic loss among all sectors. Each axis denotes an industry sector. The points on the axis denote expected losses. The number is the multiples of baseline. From this figure, it can be seen that manufacturing, transport and postal activities, electricity, gas, heat supply and water, and wholesale and retail trade were the most affected sectors in terms of property damage in Nagoya city. Among all industry sectors, climate change scenarios 1, 2, and 3, respectively, caused around 3, 3–5, and 5–7 times the expected loss in the no climate change scenario. Under the climate change scenario 3, the expected property damage in manufacturing could be more than a thousand times of loss in other industry sectors, such as finance and insurance, education, and learning support. Similar analysis was conducted for business interruption losses. Manufacturing, transport and postal activities, wholesale and retail trade, and services were the most affected sectors in terms of business loss in Nagoya city. It is worth noting that some industry sectors, such as services, accommodations, food and drinks services, medical, health care, and welfare, which do not get any attention in terms of property damage, should be given attention in terms of business interruption losses.

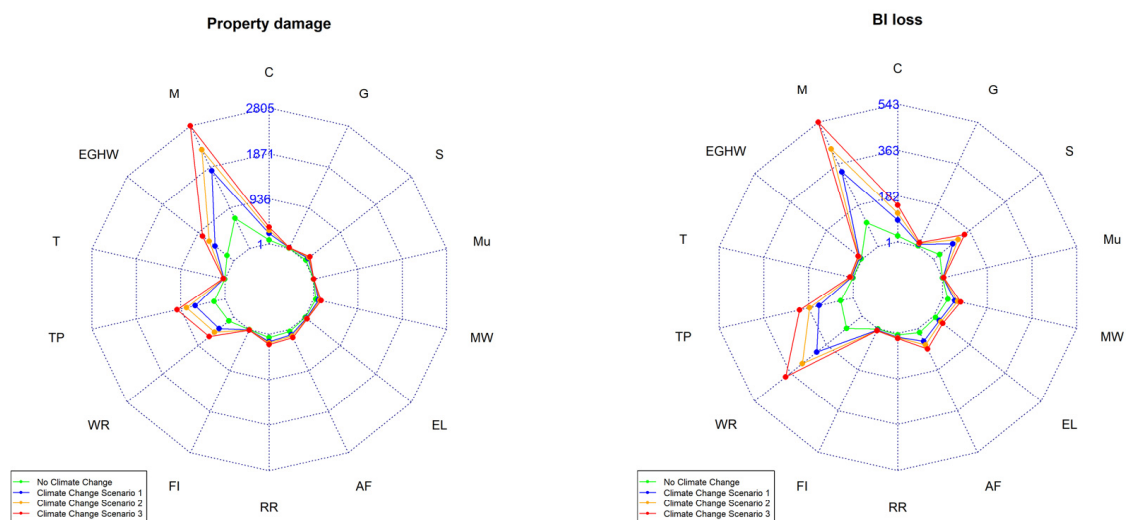


Figure 9. Property damage and business interruption in Nagoya city. (C: Construction; M: Manufacturing; EGHW: Electricity, gas, heat supply, and water; T: Information and communications; TP: Transport and postal activities; WR: Wholesale and retail trade; FI: Finance and insurance; RR: Real estate and goods rental and leasing; AF: Accommodations, eating, and drinking services; EL: Education and learning support; MW: Medical, health care, and welfare; Mu: Multiservice; S: Services; G: Government affairs).

3.3.3. Comprehensive Assessment of Vulnerable Industry Sectors in Different Areas

The vulnerable sectors could be different for different districts. A comprehensive assessment of vulnerable industry sectors in different areas were obtained using region-specific and industry-specific EP curves. With a risk and radar map, the climate change impact in industry sectors in three districts were compared. As shown in Figure 10, in Minato district, the property damage in manufacturing, electricity, gas, heat supply and water, and transport and postal activities were severe, but in Kawagoe-cho and Chita-shi, transport and postal activities were not affected as much. The manufacturing sector was the most affected sector in most districts, but in Kawagoe district, it was not as significant as electricity, gas, heat supply, and water sectors. The shape of the radar maps shows different patterns of economic impact. It was useful to cluster the areas with similar economic impact patterns. Decision makers can make similar climate change adaptation strategies in the same cluster to save on decision-making cost.

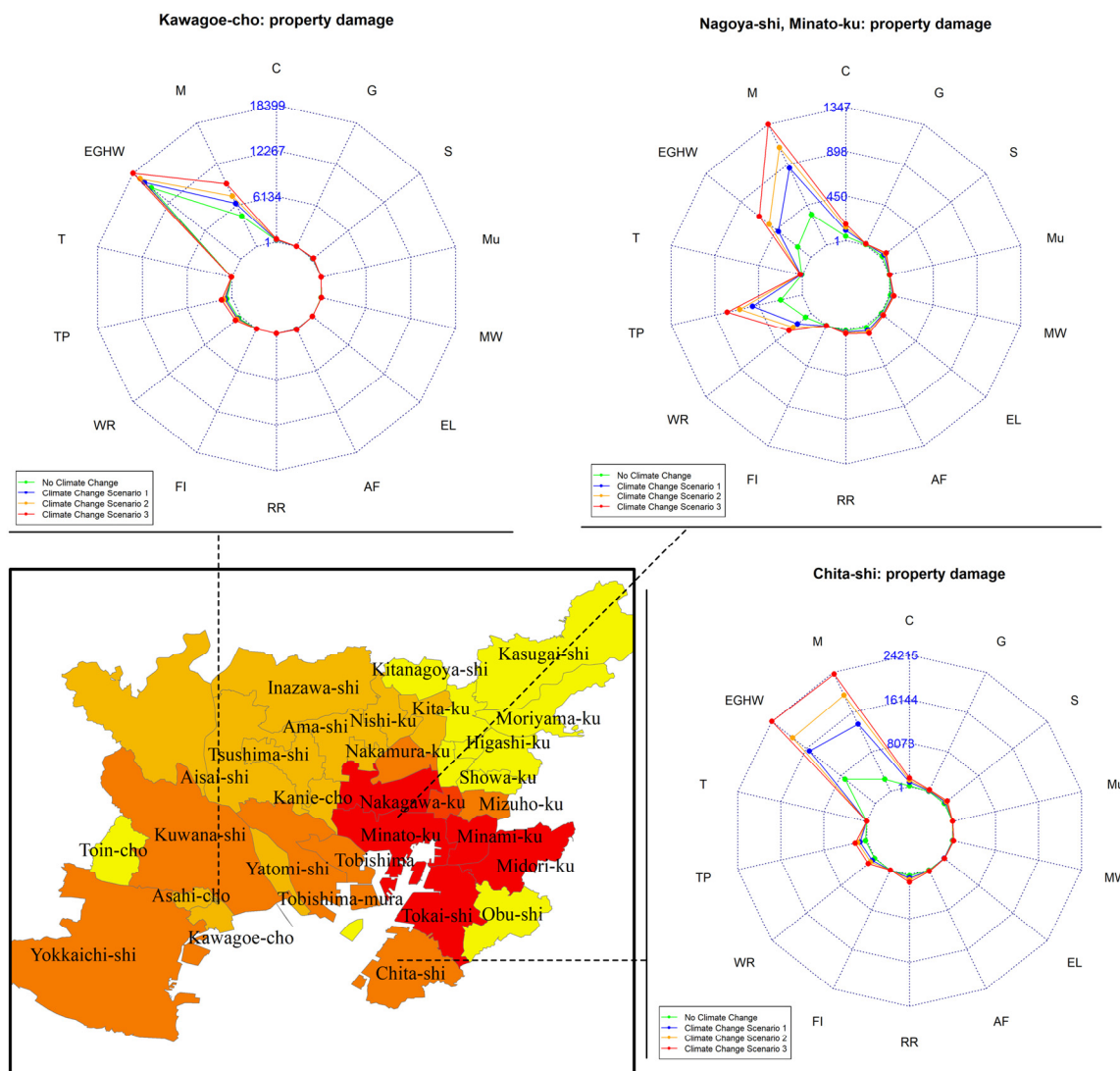


Figure 10. Property damage in different areas. (C: Construction; M: Manufacturing; EGHW: Electricity, gas, heat supply, and water; T: Information and communications; TP: Transport and postal activities; WR: Wholesale and retail trade; FI: Finance and insurance; RR: Real estate and goods rental and leasing; AF: Accommodations, eating, and drinking services; EL: Education and learning support; MW: Medical, health care, and welfare; Mu: Multiservice; S: Services; G: Government affairs).

4. Discussions

This study presents a coherent framework to quantify storm surge inundation risk due to climate change, represented by four scenarios of climate change, in the coastal area of Ise Bay, Japan. Simulation-based EP curves were created to represent the storm surge inundation risk and to analyze the economic impact of climate change. This method can provide a complete version of risk information for local decision makers to identify the changes in risky areas and vulnerable industry sectors under climate change scenarios.

Most studies investigating climate change impact on coastal regions have tended to focus on the change in hazard risk, such as predicting the change in sea level [2], number of typhoons [34], increase in storm surge height [36], and so on. These studies are significant for understanding climate change impact on the natural systems. However, to understand the climate change risk to social systems, further investigations are necessary. This study has two strengths over the previous studies: (i) Risk is defined by the probability of economic loss, which integrates the information of hazard assessment, exposure, and vulnerability of property and industry sectors for a better understanding of climate change

risk to society; and (ii) the simulation-based EP curves, developed to link the probability of hazard occurrence and the probability of economic loss, can directly shift the focus towards decision making.

In regards to the methodology proposed in this paper, the following issues should be noted. On hazard simulation, the cascading process from typhoon generation to storm surge and coastal inundation simulation is presented. The key process to construct the methodology is typhoon ensemble forecasting. All the simulations and statistical analysis are based on the typhoon generation. On loss estimation, the property damage and business interruption loss are estimated for industry sectors in this paper, because double counting can take place if they are simply added. Further, business interruption loss mentioned in this paper is the primary business interruption loss, which is caused directly by the inundation. The higher order business interruption loss caused by interruptions in the business chain is not included. The average ratio between primary business interruption loss and property damage among all sectors in the study is less than 1:10. The expected loss is used as a representation of EP curves in discussing the case study results; however, it could make the risks appear moderate [28]. EP curves provide a complete version of risk information. For different purposes, the conditional expected value or value at risk (VaR) can be used instead of the expected value.

5. Conclusions

The aim of this study is to propose a simulation-based methodology to construct EP curves and assess the economic impact to society by climate change. The case study in Ise Bay demonstrates the proposed methodology. From this research, two conclusions can be made.

The study emphasizes the significance of integration of hazard, exposure, and vulnerability. Risk is represented by EP curves that integrate the probability distribution of hazards and the probability distribution of loss caused by the hazards. Simulation is a valid method to resolve the problem of data deficiency during the construction of EP curves. The proposed methodology is feasible for application; however, cross-disciplinary cooperation from typhoon ensemble forecasting to economic loss calculation is necessary.

Through the EP curves in the case study areas, many results can be obtained. Among them, of interest in our research, three findings are highlighted: (i) The region-specific EP curves show that risk level is different among districts, and expected losses increase 3–7 times after considering climate change. In Nagoya city, the impact of high-frequency storm surges, such as a 1/50 event, are not significant with and without climate change. However, the impact of low-frequency storm surges, such as a 1/200 event, will dramatically increase after climate change. Minato district and Minami district are vulnerable to high storm surge risk, even without climate change, and the severity will increase with climate change. Nakagawa district, Midori district, and Tokai city will become high-risk areas with climate change. (ii) Industry sector-specific EP curves show that the manufacturing sector is relatively sensitive and highly susceptible to climate change in the case study area, although the situation could be different in another district. Manufacturing, transport and postal activities, electricity, gas, heat supply and water, and wholesale and retail trade are the most affected sectors in terms of property damage. Manufacturing, transport and postal activities, wholesale and retail trade, and services are the most affected sectors in terms of business interruption loss. (iii) Comprehensively using region- and industry-specific EP curves give a better understanding of vulnerable industrial sectors in different risky areas that facilitate making countermeasures and adaptation strategies for climate change.

Author Contributions: N.M. provided data and resources; H.T. and X.J. designed the methodology; L.Y. and X.J. conducted the investigation and data analysis. H.T. administrated the project. X.J. and L.Y. wrote the paper.

Funding: This work was supported under the framework of the Integrated Hazards Projections in the Integrated Research Program for Advancing Climate Models (TOUGOU Program), supported by the Ministry of Education, Culture, Sports, Science, and Technology Japan (MEXT) and Grants-in-Aid for Scientific Research Kakenhi by JSPS. This study was also supported by the National Natural Science Foundation of China (Grant No. 41807504) and Fundamental Research Funds for Central Universities (WUT: 2019VI032), China.

Conflicts of Interest: The authors declare no conflicts of interest.

References

1. Centre for Research on the Epidemiology of Disasters (CRED) & UN Office for Disaster Risk Reduction (UNISDR). Economic Losses, Poverty and Disasters 1998–2017. 2018. Available online: <https://www.unisdr.org/we/inform/publications/61119> (accessed on 1 January 2019).
2. Intergovernmental Panel on Climate Change. *Climate Change 2013: The Physical Science Basis, Working Group I Contribution to the Fifth Assessment Report of the Intergovernmental Panel on Climate Change*; Cambridge University Press: Cambridge, UK, 2014.
3. Neumann, B.; Vafeidis, A.T.; Zimmermann, J.; Nicholls, R.J. Future coastal population growth and exposure to sea-level rise and coastal flooding—a global assessment. *PLoS ONE* **2015**, *10*, e0118571. [[CrossRef](#)] [[PubMed](#)]
4. UN Office for Disaster Risk Reduction (UNISDR). Sendai framework for disaster risk reduction 2015–2030. In Proceedings of the 3rd United Nations World Conference on DRR, Sendai, Japan, 18 March 2015.
5. Tatano, H. Major Characteristics of disaster risk and its management strategies. *Sociotechnica* **2003**, *1*, 141–148. [[CrossRef](#)]
6. Wahl, T.; Jain, S.; Bender, J.; Meyers, S.D.; Luther, M.E. Increasing risk of compound flooding from storm surge and rainfall for major US cities. *Nat. Clim. Chang.* **2015**, *5*, 1093. [[CrossRef](#)]
7. Kuriqi, A.; Ardiçlioglu, M. Investigation of hydraulic regime at middle part of the Loire River in context of floods and low flow events. *Pollack Period.* **2018**, *13*, 145–156. [[CrossRef](#)]
8. Kuriqi, A. Assessment and quantification of meteorological data for implementation of weather radar in mountainous regions. *Mausam* **2016**, *67*, 789–802.
9. Zhang, S.; Li, Y.; Ma, M.; Song, T.; Song, R. Storm Water Management and Flood Control in Sponge City Construction of Beijing. *Water* **2018**, *10*, 1040. [[CrossRef](#)]
10. Gao, Y.; Wang, H.; Liu, G.M.; Sun, X.Y.; Fei, X.Y.; Wang, P.T.; He, Y.W. Risk assessment of tropical storm surges for coastal regions of China. *J. Geophys. Res. Atmos.* **2014**, *119*, 5364–5374. [[CrossRef](#)]
11. Wu, W.; Westra, S.; Leonard, M. A basis function approach for exploring the seasonal and spatial features of storm surge events. *Geophys. Res. Lett.* **2017**, *44*, 7356–7365. [[CrossRef](#)]
12. Cid, A.; Menéndez, M.; Castanedo, S.; Abascal, A.J.; Méndez, F.J.; Medina, R. Long-term changes in the frequency, intensity and duration of extreme storm surge events in southern Europe. *Clim. Dyn.* **2016**, *46*, 1503–1516. [[CrossRef](#)]
13. Harman, B.P.; Heyenga, S.; Taylor, B.M.; Fletcher, C.S. Global lessons for adapting coastal communities to protect against storm surge inundation. *J. Coast. Res.* **2013**, *31*, 790–801. [[CrossRef](#)]
14. Hallegatte, S.; Henriot, F.; Corfee-Morlot, J. The economics of climate change impacts and policy benefits at city scale: A conceptual framework. *Clim. Chang.* **2011**, *104*, 51–87. [[CrossRef](#)]
15. Yoon, J.J. Fine-resolution Numerical Simulations to Estimate Storm Surge Height and Inundation Vulnerability Considering Future Climate Change Scenario. *J. Coast. Res.* **2018**, *85*, 916–920. [[CrossRef](#)]
16. Mori, N.; Yasuda, T.; Mase, H.; Tom, T.; Oku, Y. Projection of extreme wave climate change under global warming. *Hydrol. Res. Lett.* **2010**, *4*, 15–19. [[CrossRef](#)]
17. Yang, Z.; Wang, T.; Leung, R.; Hibbard, K.; Janetos, T.; Kraucunas, I.; Wilbanks, T. A modeling study of coastal inundation induced by storm surge, sea-level rise, and subsidence in the Gulf of Mexico. *Nat. Hazards* **2014**, *71*, 1771–1794. [[CrossRef](#)]
18. Sahoo, B.; Bhaskaran, P.K. A comprehensive data set for tropical cyclone storm surge—Induced inundation for the east coast of India. *Int. J. Climatol.* **2018**, *38*, 403–419. [[CrossRef](#)]
19. Yin, J.; Lin, N.; Yu, D. Coupled modeling of storm surge and coastal inundation: A case study in New York City during Hurricane Sandy. *Water Resour. Res.* **2016**, *52*, 8685–8699. [[CrossRef](#)]
20. Li, N.; Yamazaki, Y.; Roeber, V.; Cheung, K.F.; Chock, G. Probabilistic mapping of storm-induced coastal inundation for climate change adaptation. *Coast. Eng.* **2018**, *133*, 126–141. [[CrossRef](#)]
21. Davidson, R.A.; Lambert, K.B. Comparing the hurricane disaster risk of US coastal counties. *Nat. Hazards Rev.* **2001**, *2*, 132–142. [[CrossRef](#)]
22. Zhang, J. Risk assessment of drought disaster in the maize-growing region of Songliao Plain, China. *Agric. Ecosyst. Environ.* **2004**, *102*, 133–153. [[CrossRef](#)]

23. Balica, S.F.; Wright, N.G.; Vander Meulen, F. A flood vulnerability index for coastal cities and its use in assessing climate change impacts. *Nat. Hazards* **2012**, *64*, 73–105. [[CrossRef](#)]
24. Ouma, Y.O.; Tateishi, R. Urban flood vulnerability and risk mapping using integrated multi-parametric AHP and GIS: Methodological overview and case study assessment. *Water* **2014**, *6*, 1515–1545. [[CrossRef](#)]
25. Lowrance, W.W. *Of Acceptable Risk: Science and the Determination of Safety*; William Kaufmann: San Francisco, CA, USA, 1976.
26. Haimes, Y.Y. On the definition of vulnerabilities in measuring risks to infrastructures. *Risk Anal. Int. J.* **2006**, *26*, 293–296. [[CrossRef](#)] [[PubMed](#)]
27. Haimes, Y.Y. Systems-based guiding principles for risk modeling, planning, assessment, management, and communication. *Risk Anal. Int.* **2012**, *32*, 1451–1467. [[CrossRef](#)] [[PubMed](#)]
28. Haimes, Y.Y. *Risk Modeling, Assessment, and Management*; John Wiley & Sons: Hoboken, NJ, USA, 2015.
29. Roeckner, E.; Bengtsson, L.; Feichter, J.; Lelieveld, J.; Rodhe, H. Transient climate change simulations with a coupled atmosphere-ocean GCM including the tropospheric sulfur cycle. *J. Clim.* **1999**, *12*, 3004–3032. [[CrossRef](#)]
30. Hewitson, B.C.; Crane, R.G. Consensus between GCM climate change projections with empirical downscaling: Precipitation downscaling over South Africa. *Int. J. Climatol.* **2006**, *26*, 1315–1337. [[CrossRef](#)]
31. Knutson, T.R.; McBride, J.L.; Chan, J.; Kerry, E.; Holland, G.; Landsea, C.; Held, I.; Kossin, J.P.; Srivastava, A.K.; Sugi, M. Tropical cyclones and climate change. *Nat. Geosci.* **2010**, *3*, 157–163. [[CrossRef](#)]
32. Murakami, H.; Wang, Y.; Yoshimura, H.; Mizuta, R.; Sugi, M.; Shindo, E.; Ose, T. Future changes in tropical cyclone activity projected by the new high-resolution MRI-AGCM. *J. Clim.* **2012**, *25*, 3237–3260. [[CrossRef](#)]
33. Liu, P.; Kajikawa, Y.; Wang, B.; Kitoh, A.; Yasunari, T.; Li, T.; Rajendran, K. Tropical intraseasonal variability in the MRI-20km60L AGCM. *J. Clim.* **2009**, *22*, 2006–2022. [[CrossRef](#)]
34. Yasuda, T.; Nakajo, S.; Kim, S.; Mase, H.; Mori, N.; Horsburgh, K. Evaluation of future storm surge risk in East Asia based on state-of-the-art climate change projection. *Coast. Eng.* **2014**, *83*, 65–71. [[CrossRef](#)]
35. Kim, S.Y.; Yasuda, T.; Mase, H. Numerical analysis of effects of tidal variations on storm surges and waves. *Appl. Ocean Res.* **2008**, *30*, 311–322. [[CrossRef](#)]
36. Shibutani, Y.; Kim, S.Y.; Yasuda, T.; Mori, N.; Mase, H. Sensitivity of future tropical cyclone changes to storm surge and inundation: Case study in Ise Bay, Japan. *Coast. Eng. Proc.* **2014**, *1*, 27. [[CrossRef](#)]
37. Liang, Q. Flood simulation using a well-balanced shallow flow model. *J. Hydraul. Eng.* **2010**, *136*, 669–675. [[CrossRef](#)]
38. Jiang, X.; Mori, N.; Tatano, H.; Yang, L.; Shibutani, Y. Estimation of property loss and business interruption loss caused by storm surge inundation due to climate change: A case of Typhoon Vera revisit. *Nat. Hazards* **2016**, *84*, 35–49. [[CrossRef](#)]
39. Chang, S.E.; Falit-Baiamonte, A. Disaster vulnerability of businesses in the 2001 Nisqually earthquake. *Glob. Environ. Chang. Part B Environ. Hazards* **2002**, *4*, 59–71. [[CrossRef](#)]
40. Rose, A.; Lim, D. Business interruption losses from natural hazards: Conceptual and methodological issues in the case of the Northridge earthquake. *Glob. Environ. Chang. Part B Environ. Hazards* **2002**, *4*, 1–14. [[CrossRef](#)]
41. Hallegatte, S.; Hourcade, J.C.; Ambrosi, P. Using climate analogues for assessing climate change economic impacts in urban areas. *Clim. Chang.* **2007**, *82*, 47–60. [[CrossRef](#)]
42. Kajitani, Y.; Tatano, H. Estimation of production capacity loss rate after the great East Japan earthquake and tsunami in 2011. *Econ. Syst. Res.* **2014**, *26*, 13–38. [[CrossRef](#)]
43. Yang, L.; Kajitani, Y.; Tatano, H.; Jiang, X. A methodology for estimating business interruption loss caused by flood disasters: Insights from business surveys after Tokai Heavy Rain in Japan. *Nat. Hazards* **2016**, *84*, 411–430. [[CrossRef](#)]

